

## Effect of Hydrothermal Conditions on the Morphology of Colloidal Boehmite Particles: Implications for Fibril Formation and Monodispersity

Paul A. Buining\*†, Chellappah Pathmamanoharan,† Monique Bosboom,†  
J. Ben H. Jansen,\* and Hendrik N.W. Lekkerkerker†

Department of Chemical Geology, University of Utrecht,  
Budapestlaan 4, 3508 TA Utrecht, Netherlands, and  
Van 't Hoff Laboratory, University of Utrecht, Padualaan 8, 3508 TB Utrecht, Netherlands

The synthesis of colloidal boehmite (AlOOH) is studied by heating basic aluminum chloride solutions under constant stirring. The temperature and  $\text{Al}_2\text{O}_3:\text{Cl}$  molar ratio influence the product morphology. Synthesis at  $140^\circ\text{C}$  generates highly fibrous polycrystalline particles that are on average 360 nm long, 30 nm broad, and 8 nm thick. They contain 0.11 mol of excess  $\text{H}_2\text{O}$  per 1 mol of AlOOH. Synthesis at temperatures between  $140^\circ$  and  $190^\circ\text{C}$  produces broader fibrils and less excess  $\text{H}_2\text{O}$ . Preparation at  $220^\circ\text{C}$  eventually produces fully crystalline platelike boehmite particles about 260 nm long, 95 nm broad, and 14 nm thick, without excess  $\text{H}_2\text{O}$ . Fibril synthesis requires an  $\text{Al}_2\text{O}_3:\text{Cl}$  molar ratio exceeding 1.0 to yield noncoagulated particles. The fibrils are fairly monodisperse with 20% standard deviation in their length for an  $\text{Al}_2\text{O}_3:\text{Cl}$  molar ratio about 1.0. [Key words: boehmite, colloids, fibers, hydrothermal process, birefringence.]

### I. Introduction

IN RECENT years there has been increasing interest in the synthesis of monodisperse colloidal particles of metal oxides.<sup>1,2</sup> Such dispersions are essential for the development of the theory of colloid science and are needed in catalysis and the ceramics industry. If the process conditions are controlled, uniform particles of specific shapes and sizes can be produced. Matijević<sup>3</sup> prepared various colloidal dispersions consisting of uniform particles of various chemical compositions. He recorded changes in the shapes and sizes of the particles by systematically varying the reaction conditions.

Similar to dispersions of uniform spherical silica particles, which produce transparent colloidal crystals,<sup>4</sup> monodisperse sols of fibrillar boehmite particles exhibit interesting phenomena such as streaming birefringence and lyotropic liquid phases.<sup>5</sup> These properties have scarcely been investigated because of the absence of suitable fibrillar model particles.

A method for synthesizing boehmite was originally reported by Bugosh.<sup>6</sup> Basic aluminum chloride solutions are prepared by the addition of aluminum powder to an aqueous solution of aluminum chloride. The basic aluminum chloride is diluted and treated hydrothermally. The adjective "basic" implies the presence of  $\text{Al}^{3+}$  in  $\text{OH}^-$ -bearing complexes in a solution which is, however, acid.

In the study reported here an improved autoclaving technique is applied in which the solution is mixed thoroughly

during hydrothermal treatment to obtain a monodisperse product. The influence of synthesis conditions on the length and diameter of the particles is studied by systematically varying the synthesis temperature and time, initial aluminum concentration, and  $\text{Al}_2\text{O}_3:\text{Cl}$  molar ratio.

The product was characterized by transmission electron microscopy (TEM), X-ray diffraction (XRD), electron diffraction, thermogravimetric analysis (TGA), and differential thermal analysis (DTA). The particle-size distribution was treated statistically with a computerized particle-size analyzer.

A first indication of whether or not the sol consists of non-coagulated fibrillar boehmite particles is the qualitative induction of streaming birefringence, an optical phenomenon that appears when the sol is viewed between crossed polarization filters. It is caused by parallel orientation of the particles because of velocity gradients when the sol is stirred.<sup>7</sup>

### II. Experimental Procedure

#### (1) Materials

Aluminum powder<sup>†</sup> and aluminum chloride hexahydrate ( $\text{AlCl}_3 \cdot 6\text{H}_2\text{O}$ )<sup>‡</sup> were used as supplied. Double-distilled water was used throughout the experiments.

#### (2) Preparation of the Basic Aluminum Chloride Solution

The method for making the basic aluminum chloride stock solutions was described by Bugosh<sup>6</sup> and was recently reinvestigated by Brusasco *et al.*<sup>8</sup> and Sterte *et al.*<sup>9</sup> Aluminum powder was added under vigorous stirring to an aqueous solution of  $\text{AlCl}_3 \cdot 6\text{H}_2\text{O}$  at  $70^\circ\text{C}$  contained in a vessel that was connected to a condenser to prevent loss of water. Solutions of various  $\text{Al}_2\text{O}_3:\text{Cl}$  molar ratios (denoted by A:C) were prepared by varying the amount of aluminum powder.

The aluminum powder was added in portions of 1 g; it took a few days for each portion to dissolve. The final stock solutions with an A:C ratio up to 1.0 contained 1.0 mol/L of  $\text{Cl}^-$ . For the higher A:C ratios additional dilution appeared to be necessary to reduce gelation, resulting in a solution of 0.5 mol/L of  $\text{Cl}^-$ . When the A:C ratio reached about 1.5, any further addition of aluminum powder did not dissolve.

All stock solutions were cloudy because of condensation of probably an amorphous aluminum hydroxide. Solutions with an A:C ratio larger than about 1.0 were gray colored and had a thixotropic rheology.

After dilution of the basic aluminum chloride solutions to an identical  $\text{Cl}^-$  concentration of 0.05 mol/L, pH measurements gave values varying from 3.8 for a solution with an A:C ratio of 0.5, to a value of 4.4 in the case of an A:C ratio of 1.5.

L. Klein—contributing editor

Manuscript No. 198041. Received October 20, 1989; approved March 6, 1990.

\*Department of Chemical Geology.

†Van 't Hoff Laboratory.

‡Pulverized to 100 to 200  $\mu\text{m}$ , purity greater than 99%, Fluka AG., Buchs, Switzerland.

§Crystallized, purity greater than 99.0%, Fluka AG.

### (3) Process Conditions of Boehmite Synthesis

The boehmite sols were prepared by filling 8-mL or 44-mL Teflon<sup>1</sup> cups with the diluted basic aluminum chloride solutions. The cups were fitted into steel autoclaves and heated in a "rocking system." The autoclaves were fastened to a framework which rotated at a constant velocity of 5.75 rpm in an oven at a certain temperature. The rotation of the autoclave produced a constant and thorough mixing of the solution, which prevented gradients in temperature as well as in molecular species and particle concentrations. Under the conditions of heating, the vapor pressure within the autoclave, which was 80% filled, ranged from about 0.5 MPa at 150°C to about 2.3 MPa at 220°C, as determined from the theoretical diagram.<sup>10</sup> The synthesis time was varied from 4 to 55 h.

### (4) Characterization Techniques

The specimen for TEM was prepared by spraying the diluted sol with a nebulizer onto freshly split mica. A thin carbon layer was deposited upon the mica plate by evaporation in a vacuum chamber. The carbon layer, bearing the boehmite particles, was separated from the mica on water (the carbon floats) and was transferred to a copper, 400-mesh carrier grid. The grid was placed in a transmission electron microscope, \*\* having an accelerating voltage of 100 kV. Both electron microscopy and electron diffraction were performed on the same grid. The highest magnification was 11 000 times.

XRD patterns of samples were obtained using monochromatic  $\text{CuK}\alpha_1$  radiation with a Guinier camera.<sup>11</sup>

The TGA measurements of weight loss as a function of temperature of some boehmite powders was conducted using a thermal analyzer<sup>12</sup> at a heating rate of 10°C/min. DTA was also performed on the thermal analyzer, heating at 20°C/min. In both cases the atmosphere was nitrogen, flowing at 50 mL/min.

## III. Results and Discussion

Tables I to IV list a selection of 12 out of about 90 experiments done under several variations in treatment conditions, namely temperature, A:C ratio, time, and  $\text{Cl}^-$  concentration. TEM micrographs (Fig. 1) of experiments 2, 3, 4, and 5 illustrate the steps in the treatment temperature between 155° and 220°C (see also Table I). At 155°C (Fig. 1(A)) the boehmite particles are irregularly shaped fibrils about 270 nm long, 30 nm broad, and 8 nm thick. The fibrils are predominantly oriented on their flat faces on the TEM grid. Consequently the aspect ratio (length:width ratio) is defined. There are only a few tilted fibrils, from which the particle thickness can be determined. It is striking that the boehmite fibrils are polycrystalline, being built up of very small identically oriented crystallite units about 40 nm long, 10 nm broad, and 8 nm thick. With high-resolution TEM the widely spaced (010) lattice fringes are visible parallel to the elongation of

the particle when the particle is tilted parallel to the electron beam.

At growth temperatures of 175°C and up to 190°C (Figs. 1(B) and 1(C)) the fibrils become broader, thicker, and clearly more crystalline than those formed at 155°C. They are built up of increasingly fewer crystallite units, which have become more and more crystalline and are about 150 nm long and 40 nm broad.

The particles grown at 220°C are no longer polycrystalline (Fig. 1(D)), but they are well-crystallized, broad, and thick bladelike boehmite particles, about 260 nm long, 95 nm broad, and 14 nm thick. Occasionally they are twinned. Synthesis at temperatures lower than about 120°C results in the presence of large pseudo-hexagonal boehmite plates up to 300 nm as a byproduct.

Particle length and aspect ratio distributions of the monodisperse fibrillar boehmite sol of experiment 8 display, in histograms, lognormal distributions that level out toward high values (Fig. 2). The few, extremely long fibrils around 800 nm, which are about twice the average length, occur in all dispersions of fibrillar boehmite. Because of the skewness of the distributions of the length and aspect ratio, their average values are shifted to values which are somewhat higher than their frequency maxima. The particle width distribution is irregular with deviations from low to high values, and the distribution seems to be polymodal. The maxima of the various populations of the particle width at 11, 20, 27, 41, and 54 nm may be attributed to layer repetitions of particles that are from one to a maximum of about five crystallite units broad. The units grown at 150°C have a width of about 10 nm (Table I), which seems to match the intervals between the statistical maxima. The frequency maximum at about 27 nm may indicate that a width of three units is favored under the conditions of experiment 8. Experiment 7 (155°C, A:C = 1.0) shows standard deviations of 20% for the fibril length and 33% for its width, a degree of monodispersity which could not be improved under the present conditions. The fibril uniformity may, however, more or less be influenced by various deviations (such as impurities) from the intended process conditions.

After solutions with A:C ratios less than about 1.0 were treated at 155°C, the fibrils coagulated strongly in juxtaposition. The result of experiment 6 with an A:C ratio of 0.7 illustrates this coagulation (Fig. 3(A)). The treatment of an A:C = 1.2 solution in experiment 2 at the same temperature leads to considerably less coagulation and, therefore, better monodispersity than that in experiment 6 (Fig. 3(B)). Because the solutions treated in experiments 2 and 6 had the same  $\text{Cl}^-$  concentration, the difference in morphology of the particles is not expected to be caused by a change in thickness of the  $\text{Cl}^-$ -bearing electric double layer around the boehmite during synthesis. However, a certain amount of the  $\text{Cl}^-$  ions might participate in aluminum complexes in solution, with different behaviors for different A:C ratios.

A rising A:C ratio correlates positively with an increasingly needlelike shape of the particles, expressed by the aspect ratios (see Table II).

The electron diffraction pattern (inset of Fig. 3(A)) specific for finely grown fibrillar boehmite (experiment 6) consists of

Table I. Variation in the Average Particle Dimensions with Temperature of Heating\*

Experiment No.	Heating temperature (°C)	n	Particle length (nm)	Particle width (nm)	Aspect ratio	Thickness (nm) <sup>†</sup>	Crystallite units (nm) <sup>†</sup>	
							Length	Width
1	140	30	358 [32]	30 [43]	14.5 [68]	nd	nd	nd
2	155	76	273 [30]	33 [39]	9.0 [37]	8	25–55	7–14
3	175	62	322 [49]	47 [36]	7.1 [42]	nd	40–70	14–25
4	190	38	279 [48]	51 [24]	5.4 [37]	nd	80–200	25–55
5	220	37	255 [33]	94 [23]	2.8 [36]	14	160–400	70–110

\*Standard deviation percentages in brackets. With the estimated dimension intervals of the crystallite units that build up a particle. The number of measured particles is given by n. A:C = 1.2, 0.05 mol/L of  $\text{Cl}^-$ , length of treatment is 20 h. †nd is not determined.

<sup>1</sup>E. I. du Pont de Nemours & Co., Wilmington, DE.

<sup>2</sup>Model CM-10, Philips Electronic Instruments, Inc., Mahwah, NJ.

<sup>3</sup>Model FR 522, Enraf Nonius, Delft, Netherlands.

<sup>4</sup>Model 1090, E. I. du Pont de Nemours & Co.

**Table II. Variation in the Average Particle Dimensions with A:C Ratio\***

Experiment No.	Molar ratio, A:C	Heating temperature (°C)	n	Particle length (nm)	Particle width (nm)	Aspect ratio
6	0.7	155	22	461 [28]	122 [52]	4.3 [42]
7	1.0	155	48	383 [20]	49 [33]	8.3 [29]
2	1.2	155	76	273 [30]	33 [39]	9.0 [37]
8	1.5	150	123	287 [45]	29 [38]	11.2 [64]
9	0.7	190	27	332 [47]	93 [44]	3.7 [46]
4	1.2	190	38	279 [48]	51 [24]	5.4 [37]

\*Standard deviation percentages in brackets. The number of measured particles is represented by n. 0.05 mol/L of Cl<sup>-</sup>, length of treatment is 20 h.

concentric circles. This confirms that the fibrils are oriented randomly with their (010) faces on the TEM grid.

The fibrils synthesized up to 55 h (Table III) already show a fixed length and width after 4 h. The shape of the fibrils remains practically unchanged upon longer treatment. The AlOOH yield increases with the synthesis time (Table IV). When the true boehmite yield is calculated, the amounts of adsorbed and crystal water, obtained with TGA and DTA measurements, are subtracted from the total weight of boehmite in solution. Heating for 20 h at 140°C yields 64% of the maximum achievable boehmite yield, compared with 33% after 4 h at 140°C. Synthesis for 20 h at 190°C produces 30% more boehmite than that for 20 h at 140°C. Because the fibril morphology is already fixed after a few hours of treatment, whereas boehmite growth still continues according to the yield results, one can postulate a certain mechanism for boehmite formation. A particular fibril completes its growth within a very short time, probably within 1 h. A qualitative explanation is the growth of small crystallite units, followed by fast coagulation of these units, constructing the final fibril. The generation of units is much slower and continues for about 20 h or more. This mechanism does not follow the principle of homogeneous precipitation,<sup>11</sup> which is considered to be required for the formation of uniform particles. Further work seems necessary to elucidate the exact mechanism of boehmite growth.

The aluminum concentration of the starting solution (with a certain A:C ratio) has no serious effect on the particle morphology or degree of coagulation. A Cl<sup>-</sup> concentration as high as 0.5 mol/L produces a precipitate of a poorly crystalline but very strongly agglomerated product, which still displays an electron diffraction pattern indicative of a boehmite lattice.

The pH value of the final boehmite sols ranges between about 1.1 and 1.6; there is a general trend toward a lower pH with increasing temperature of heating or longer duration of treatment. When placed between crossed polarization filters, sols containing monodisperse, noncoagulated boehmite fibrils display a streaming birefringence upon shaking or stirring. The relaxation time of the birefringence is about 5 s for a sol containing 0.5 wt% highly fibrillar boehmite and 0.05 mol/L of Cl<sup>-</sup> anions. The time can be nearly doubled by the removal of the Cl<sup>-</sup> ions by dialysis in a cellulose tube in distilled water, which also hinders flocculation of the fibrils. Dialysis for 1 week increases the pH of the sol from about 1.5 to about 6. The colloidal solutions of thick platelike particles cannot be

stabilized. The improved streaming birefringence and higher stability of a deionized fibrillar sol can be explained in terms of the DLVO theory.<sup>12,13</sup> Because of the Cl<sup>-</sup> removal, the Cl<sup>-</sup>-bearing repulsive diffusive double layers around the fibrils thicken. The more extensive repulsion between the particles prevents aggregation and forces the particles more easily into an ordered arrangement.<sup>14,15</sup> The mass of the thick platelike particles probably causes them to sink to the bottom.

In the powder XRD pattern (Fig. 4), the thick platelike particles generated at 220°C (experiment 5) reflect spacings and intensities characteristic of the highly crystalline boehmite grown hydrothermally by Christoph *et al.*<sup>16</sup> at 300°C. This result fits well to the theoretical XRD pattern they computed for a perfectly ordered boehmite lattice with space group *Amam*. In the pattern of the product made at 190°C (experiment 4) some diffraction peaks become broader, whereas in the pattern of the polycrystalline fibrils grown at 140°C (experiment 1) they may even disappear. A specific decrease in the integrals of the reflection peaks with high "k", such as (151), (080), and (231), is thereby observed. The spacing of the (020) reflection of the fibrils grown at 140°C is about 0.045 nm (0.45 Å) broader than that of the platelike product formed at 220°C. The XRD pattern of fibrillar boehmite formed by synthesis at 140°C displays the broad reflection peaks of "pseudoboehmite,"<sup>17</sup> which is generally referred to as a poorly crystalline boehmite containing excess water. Tettenhorst *et al.*<sup>18</sup> reported that the production of pseudoboehmite and boehmite depended on the temperature of the synthesis. The increase in the spacing of the (020) reflection of fibrillar boehmite compared with the platelike product probably implies the presence of excess H<sub>2</sub>O molecules in the (010) interlayer between the octahedral layers.

The powders obtained from experiments 1, 4, and 5 give different TGA and DTA patterns (Fig. 5), which confirms the presence of excess water in the fibrillar boehmite. The low-temperature DTA endothermic peak centered at about 100°C in the pattern of experiment 1 is attributed to the presence of physically bound adsorbed water on the fibrillar boehmite particles. In the case of the platelike boehmite of experiment 5 the peak is located at about 70°C and has an extremely low intensity.

The platelike product remains constant in weight over the approximate temperature range of 100° to 450°C. At 450°C the DTA registers the beginning of a sharp intense endothermic reaction which indicates instantaneous dehydration to Al<sub>2</sub>O<sub>3</sub> with a total loss of stoichiometrically bound water.

**Table III. Variation in the Average Particle Dimensions with the Time of Treatment\***

Experiment No.	Heating time (h)	n	Particle length (nm)	Particle width (nm)	Aspect ratio
10	4	132	291 [44]	31 [33]	10.8 [57]
2	20	76	273 [30]	33 [39]	9.0 [37]
11	55	72	310 [48]	35 [31]	9.4 [61]

\*Standard deviation percentages in brackets. The number of measured particles is given by n. A:C = 1.2, 0.05 mol/L of Cl<sup>-</sup>, temperature of 155°C.

**Table IV. Yields of AlOOH Originated from Total Aluminum in Solution, Calculated from Final Concentrations of Boehmite\***

Experiment No.	Heating temperature (°C)	Heating time (h)	Boehmite concentration (g/L)	AlOOH yield (%)
12	140	4	2.72	33
1	140	20	5.24	64
4	190	20	6.33	83

\*A:C = 1.2, 0.05 ml/L of Cl<sup>-</sup>.

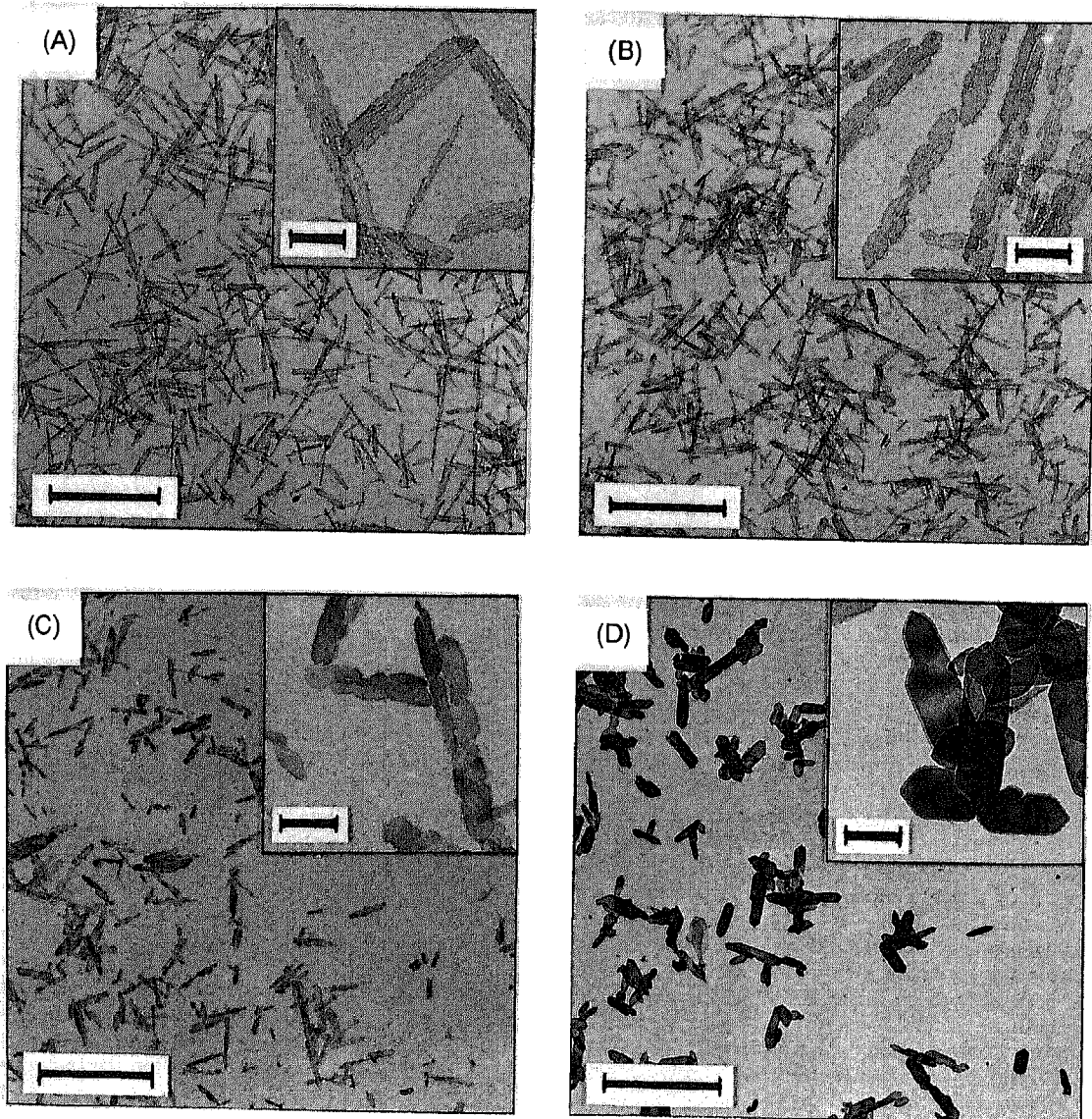


Fig. 1. TEM micrographs displaying the effect of temperature on the boehmite particle shape in (A) experiment 2 at 155°C, (B) experiment 3 at 175°C, (C) experiment 4 at 190°C, and (D) experiment 5 at 220°C. The lengths of the bars at low magnification represent 1  $\mu\text{m}$ , at high magnification in the insets, 0.1  $\mu\text{m}$ .

The TGA of the fibrillar particles already registers the loss of chemically bound water immediately after or even simultaneously with the loss of adsorbed water. At 330°C this loss begins to increase faster, which indicates a total dehydration to the final oxide. This type of dehydration leads to an endothermic peak in the DTA, which is obviously broader than that of the platelike product. From the TGA pattern a value of 0.11 mol of excess  $\text{H}_2\text{O}$  per 1 mol of  $\text{AlOOH}$  is calculated

for the fibrils of experiment 1. The particles of experiment 4 reach 0.02 mol of  $\text{H}_2\text{O}$  per 1 mol of  $\text{AlOOH}$ ; the platelike product of experiment 5 contains no excess  $\text{H}_2\text{O}$ . Baker *et al.*<sup>19</sup> postulated that the excess  $\text{H}_2\text{O}$  in pseudoboehmite was bound as terminal water, attached to  $\text{Al}^{3+}$  ions at the crystal surface. Terminal water could also participate in the excess water because the fibrils are polycrystalline and, therefore, display a large terminal area.

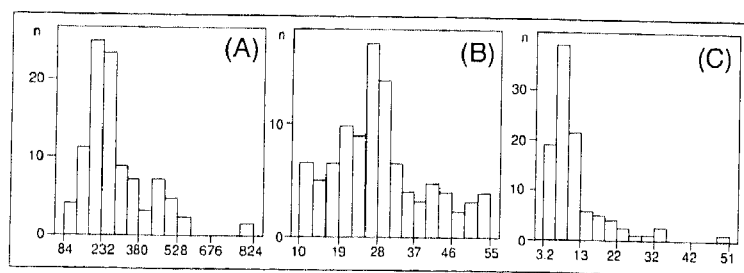


Fig. 2. Histograms of the distribution of boehmite crystal (A) lengths and (B) widths (both in nanometers), and (C) aspect ratios of the sol prepared in experiment 8.

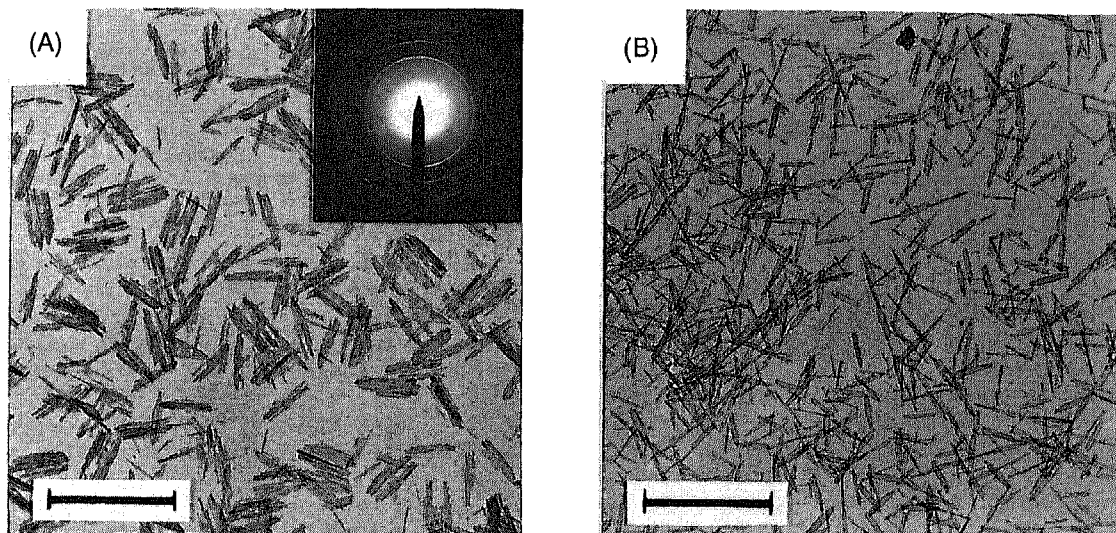


Fig. 3. TEM showing the effect of the  $Al_2O_3:Cl$  molar ratio on the coagulation of boehmite in (A) experiment 6 with  $A:C = 0.7$  and (B) experiment 2 with  $A:C = 1.2$ . The inset in (A) shows the electron diffraction pattern of the sample of experiment 6. The lengths of the bars are  $1 \mu m$ .

IV. Conclusions

Highly fibrillar submicrometer-sized boehmite particles of reasonable monodispersity, with a standard deviation of about 20% in their length, can be produced at a temperature of synthesis between  $140^\circ$  and  $160^\circ C$ , the initial solution having an  $Al_2O_3:Cl$  molar ratio of about 1.0.

Within this temperature range an increasing  $Al_2O_3:Cl$  molar ratio leads to an increasing aspect ratio of the fibrils.

Synthesis at temperatures above this range demonstrates a gradual transition of the particle morphology from strongly polycrystalline fibrils to platelike, thick boehmite particles which grow at  $220^\circ C$ .

It is not the particle length but typically the average width which correlates with temperature of formation.

Compared with the platelike particles resulting from high-temperature treatment, the fibrils have a less-ordered crystal lattice, and they are more easily dehydrated to  $Al_2O_3$ .

The  $Cl^-$  concentration of the initial solution has no effect on the particle morphology. However, a concentration approaching 0.5 mol/L might induce a precipitation of a heavily coagulated product.

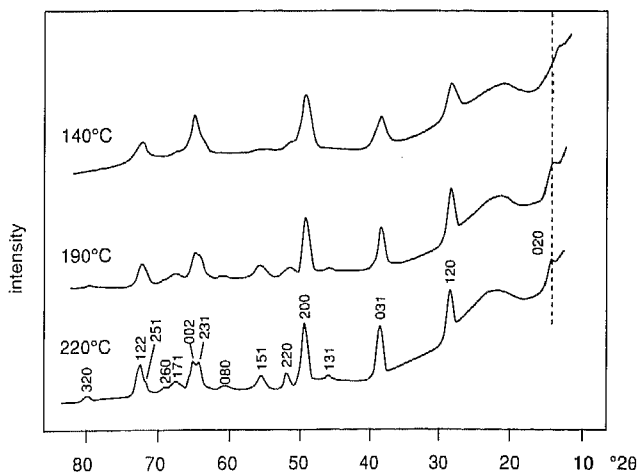


Fig. 4. Powder XRD patterns of the boehmite resulting from experiment 1 at  $140^\circ C$ , experiment 4 at  $190^\circ C$ , and experiment 5 at  $220^\circ C$ , with indexing of the reflections.

Synthesis at  $140^\circ C$  requires 20 h to produce a boehmite yield of 64%. The growth of the fibrils happens by coagulation of smaller units. This seems to occur rapidly in relation to the nucleation of the crystallite units, but more investigation is needed.

The noncoagulated, monodisperse, fibrillar system gives a stable colloidal solution after most of the  $Cl^-$  is removed from the solvent. The deionized fibrillar sols display a well-developed streaming birefringence.

**Acknowledgments:** The authors thank J. Pieters for his excellent TEM photography, A. M. J. van der Eerden for assisting with the hydrothermal equipment, H. M. V. C. Govers for XRD, T. Zalm for TGA/DTA, Dr. M. Terlou for providing a computer program for particle-size analysis, and J. L. den Boesterd for the illustrations. Thanks also to Mrs. McNab and T. Kloprogge for criticizing the text.

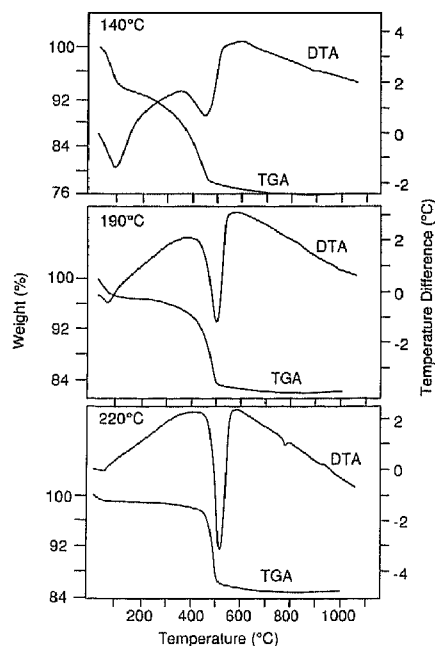


Fig. 5. TGA and DTA patterns of the boehmite powders from experiment 1 at  $140^\circ C$ , experiment 4 at  $190^\circ C$ , and experiment 5 at  $220^\circ C$ .

## References

- <sup>1</sup>E. Tani, M. Yoshimura, and S. Sōmiya, "Formation of Ultrafine Tetragonal ZrO<sub>2</sub> Powders under Hydrothermal Conditions," *J. Am. Ceram. Soc.*, **66** [1] 11–14 (1983).
- <sup>2</sup>M. Mizuno and H. Saito, "Preparation of Highly Pure Fine Mullite Powder," *J. Am. Ceram. Soc.*, **72** [3] 377–82 (1989).
- <sup>3</sup>E. Matijević, "Production of Monodisperse Colloidal Particles," *Ann. Rev. Mater. Sci.*, **15**, 483–516 (1985).
- <sup>4</sup>C. Pathmamanoharan, "Preparation of Monodisperse Polyisobutene Grafted Silica Dispersion," *Colloids Surf.*, **34**, 81–88 (1988).
- <sup>5</sup>H. Zoher and C. Török, "Tactosols," *Kolloid-Z.*, **170** [2] 140–44 (1960); **173** [1] 1–7 (1960); **180** [1] 41–51 (1961).
- <sup>6</sup>J. Bugosh, "Fibrous Alumina Monohydrate and its Production," U.S. Patent No. 2915 475, Dec. 1959.
- <sup>7</sup>H. A. Scheraga and R. Signer, *Physical Methods of Organic Chemistry—Technique of Organic Chemistry*, Vol. I, Part III; p. 2387. Edited by A. Weissberger. Interscience Publishers, New York, 1960.
- <sup>8</sup>R. Brusasco, J. Gnassi, C. Tatian, J. Baglio, K. Dwight, and A. Wold, "Preparation and Characterization of Fibrillar Boehmite and  $\gamma$ -Al<sub>2</sub>O<sub>3</sub>," *Mater. Res. Bull.*, **19**, 1489–96 (1984).
- <sup>9</sup>J. P. Sterte and J.-E. Otterstedt, "A Study on the Preparation and Properties of Fibrillar Boehmite," *Mater. Res. Bull.*, **21**, 1159–66 (1986).
- <sup>10</sup>J. R. Fisher, "The Volumetric Properties of H<sub>2</sub>O—A Graphical Portrayal," *J. Res. U.S. Geol. Surv.*, **4** [2] 189–93 (1976).
- <sup>11</sup>H. H. Willard and N. K. Tang, "A Study of the Precipitation of Aluminum Basic Sulfate by Urea," *J. Am. Chem. Soc.*, **59**, 1190–96 (1937).
- <sup>12</sup>B. V. Deryagin and L. Landau, "Theory of the Stability of Strongly Charged Lyophobic Sols and of the Adhesion of Strongly Charged Particles in Solutions of Electrolytes," *Acta Physicochim. URSS*, **14**, 633–62 (1941).
- <sup>13</sup>E. J. W. Verwey and J. T. G. Overbeek, *Theory of the Stability of Lyophobic Colloids*; pp. 41–46. Elsevier, Amsterdam, Netherlands, 1948.
- <sup>14</sup>I. Langmuir, "The Role of Attractive and Repulsive Forces in the Formation of Tactoids, Thixotropic Gels, Protein Crystals, and Coacervates," *J. Chem. Phys.*, **6**, 873–96 (1938).
- <sup>15</sup>L. Onsager, "The Effects of Shape on the Interaction of Colloidal Particles," *Ann. N.Y. Acad. Sci.*, **51**, 627–59 (1949).
- <sup>16</sup>G. G. Christoph, C. E. Corbató, D. A. Hofmann, and R. T. Tettenhorst, "The Crystal Structure of Boehmite," *Clays Clay Miner.*, **27** [2] 81–86 (1979).
- <sup>17</sup>P. H. Hsu, "Effects of Salts on the Formation of Bayerite Versus Pseudo-boehmite," *Soil Sci.*, **103** [2] 101–10 (1967).
- <sup>18</sup>R. T. Tettenhorst and D. A. Hofmann, "Crystal Chemistry of Boehmite," *Clays Clay Miner.*, **28** [5] 373–80 (1980).
- <sup>19</sup>B. R. Baker and R. M. Pearson, "Water Content of Pseudoboehmite: A New Model for its Structure," *J. Catal.*, **33**, 265–78 (1974). □